CONEM 2016
CONGRESSO NACIONAL DE ENGENHARIA MECÂNICA
21 - 25 AGOSTO DE 2016
FORTALEZA - CEARÁ

Dynamic Performance Enhancement and Singularities Suppression by the use of Kinematic Redundancy in Parallel Kinematic Manipulators

João Cavalcanti Santos, joao.cavalcanti.santos@usp.br[1]
Maíra Martins da Silva, mairams@sc.usp.br[2]
Escola de Engenharia de São Carlos - Universidade de São Paulo

Abstract: *Parallel kinematic machines present several advantages over serial architectures as higher rigidity, improved speed/torque ratio and better load capacity. However, they may suffer from singularity issues and limited workspace. The reconfiguration capability provided by kinematic redundancy can be seen as a promising alternative to reduce these drawbacks. On the other hand, its implementation requires a considerable increase of the mass and number of moving parts. A numerical analysis is proposed to assess the effectiveness of adding one or more level of kinematic redundancies to reduce the occurrence of singularity, enlarge the workspace and improve the speed/torque ratio. The non-redundant planar 3RRR manipulator is used as the basic configuration. The understudy redundant manipulators are characterized by the addition of one, two or three prismatic active joints, yielding the (P)RRR+2RRR, 2(P)RRR+RRR and 3(P)RRR planar manipulators. Based on Lagrangian formulation of mechanics, a complete rigid-body model is presented (including Inverse and Forward Dynamics) and a proper numerical method capable of integrating the resulting DAE problem is exposed. Motion planning strategies are proposed to enable the reconfiguration capability of the redundant manipulators. Gathering all analytical methods, simulations considering control systems and disturbances can be established. The consequent study compare influences of the system characteristics, mainly the redundancy. According to numerical results, one can conclude that kinematic redundancy can be an alternative to remove singularities of the workspace and improve the system dynamic performance. Nevertheless, this improvement can only be achieved by the selection of a proper motion planning strategy.*
Keywords: *Parallel Manipulators, Kinematic Redundancy, Singularities, Dynamic Performance.*

1. INTRODUCTION

Parallel Kinematic Machines (PKM) receive increasing attention since its beginnings dated to the patent of the Stewart Platform (Stewart, 1965). Using six kinematic chains with linear actuators connecting in parallel the ground basis to the moving platform, the 6 DOF mechanism has high accuracy and ability to generate high accelerations. As discussed in (Merlet, 2012), the application of parallel architecture provides higher rigidity, acceleration capabilities, accuracy and ratio between carried mass and robot mass. These characteristics rise from the fact that loads are shared among the several kinematic chains and errors read by actuators are averaged instead of accumulated (as is the case of a serial robot). The accuracy of analogous manipulators representing parallel and serial architecture is compared objectively in (Briot and Bonev, 2007), clarifying the abovementioned advantage.

In spite of these promising conditions, poor isotropicity is a serious concern (Gogu, 2007; Gosselin and Angeles, 1990; Bonev *et al.*, 2003), that is to say, loads required for movements about different directions are highly dissimilar. The worst case of this scenario is for positions in which necessary loads tends to infinity, i.e. the mechanism is unable to stay steady regardless the capacity of its actuators (complete loss of rigidity). These positions, called singular positions, are studied in (Gosselin and Angeles, 1990; Bonev *et al.*, 2003). With this in mind, great effort is applied in order to design PKMs with enhanced isotropicity (Wenger and Chablat, 2007; Gogu, 2007). In addition, as a result of constraints imposed by the multiple kinematic chains connecting the base to the moving platform, parallel manipulators usually have reduced workspace.

In this situation, redundancy can be proposed. Three cases of this concept are detailed in (Merlet, 2012):

- (A) Measurement redundancy: number of actuators is greater than the number of DOF of the mechanism. Used mainly to improve accuracy;
- (B) Actuation redundancy: Number of actuators is greater than the number of DOF of the mechanism. Robot is overconstrained, distribution of actuators loads can be optimized;

- (C) Kinematic redundancy: Number of DOF of the mechanism is greater than the number of DOF of the end-effector. There are infinite possibilities of actuators positions for a given position of the end-effector.

Focused on enhancing isotropicity, cases (B) and (C) are appropriate. Examples of planar 3 DOF manipulators are introduced in Fig. 1. Nomenclature indicates rotary joints by R and prismatic joints (or linear) by P, being underlined in case it is active. The number before letters shows the amount of kinematic chains. This way, (a) 3RRR is a manipulator with 3 kinematic chains, each one with three rotary joints, of which the first is active. This is a planar non-redundant robot with 3 DOF. Examples (b) and (c) have 4 and 6 actuators while the mechanism presents the same 3 DOF, setting cases of actuation redundancy. On the other hand, (d), (e) and (f) have more DOF (4, 5 and 6, respectively) than the end-effector (3 DOF), which establish cases of kinematic redundancy.

Actuation redundancy provides infinite possibilities of actuators loads for a given task, which should be homogenized after an optimization process. Indeed, studies show that enhanced isotropicity and higher acceleration capabilities can be attained (Corbel *et al.*, 2010; Kock and Schumacher, 1998). In (Corbel *et al.*, 2010), different degrees of actuation redundancy in Delta-like robots are cogitated, concluding that one degree of redundancy is the most appropriate for this specific circumstance. Correspondingly, (Kock and Schumacher, 1998) deduced that stiffness might be increased as well. However, as a consequence of the additional kinematic constraints, workspace may be reduced even more, as shown by (Rocha and da Silva, 2013) for configurations in Fig. 1. Furthermore, if each actuator is controlled independently, unpredicted high internal loads may occur in an overconstrained mechanism.

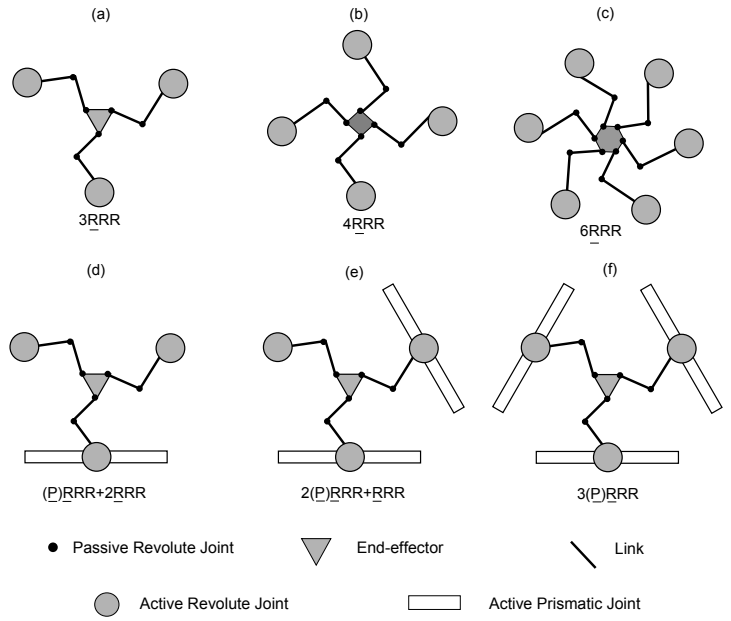

Figure 1: Non-redundant and redundant manipulators: (a) 3RRR, (b) 4RRR, (c) 6RRR, (d) PRRR+2RRR (e) 2PRRR+RRR and (f) 3PRRR

Alternatively, kinematic redundancy allows additional mobility to the manipulator, increasing its workspace. Moreover, once infinite actuators positions are admissible for a given end-effector pose, some decision process may avoid the occurrence of singularities and points of poor isotropicity. This subjects are discussed in (Ebrahimi *et al.*, 2007) focused on the robot 3PRRR.

Yet, how kinematic redundancy may deal with its extra DOF so that singularities are suppressed and loads are homogenized (in brief: enhanced dynamic performance) is still unclear. Additional actuators increase moving inertia, which may constrain the performance improvement. Additionally, how the additional mobility should be managed need to be defined.

Therefore, a complete mathematical model (including Inverse and Forward Dynamics) of the robot 3PRRR is proposed, together with a brief description of a motion planning strategy. For sake of comparison, these methods are applied in a non-redundant 3RRR and in a kinematically redundant 3PRRR.

2. MATHEMATICAL MODEL

In order to simulate the manipulator and to design its parts and control, kinematic dynamic models are necessary. These methods are presented in sections 2.1 and 2.2, respectively.

2.1 Kinematic Model

Geometric variables of the manipulator 3PRRR are depicted in Fig. 2. For every description, subindex i represents the kinematic chain of a given parameter, receiving values from 1, 2 or 3. Lengths of links A_iB_i and B_iC_i are, respectively, l_2

and l_3. There are rotary actuators in each point A_i positioning θ_i and linear actuators positioning ζ_i. Angles γ_i represent orientation of each linear actuator. Joints B_i and C_i are passive revolute joints. Length h is the distance between the center of the end-effector and any point C_i. Cartesian postion and orientation of the end-effector are given by x, y e α. The distance between the center of the manipulator (which defines the origin of the coordinate system (x, y)) and the center of any linear actuator is a. Orientation of a link B_iC_i is β_i.

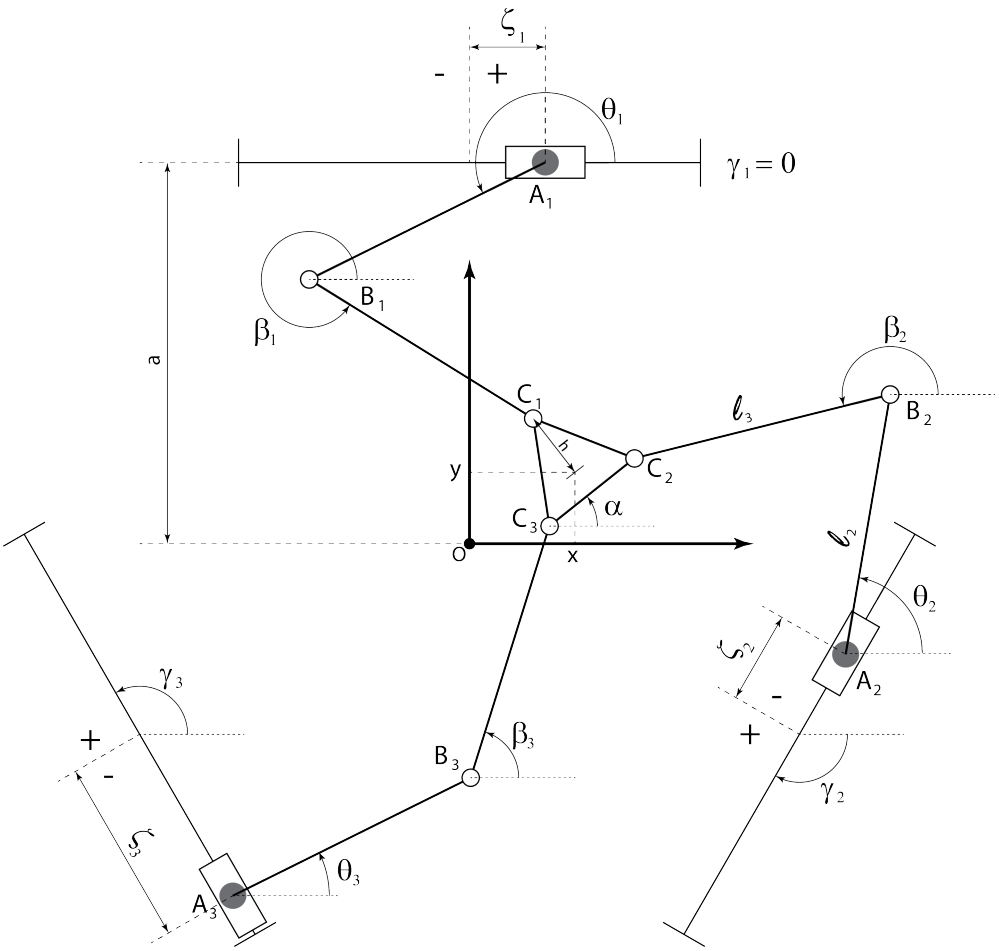

Figure 2: Schematic representation of 3PRRR

2.1.1 Inverse Kinematics

The kinematic model should correlate actuators positions $\mathbf{\Theta} = [\theta_1, \theta_2, \theta_3, \zeta_1, \zeta_2, \zeta_3]^T$ with end-effector positions $\mathbf{X} = [x, y, \alpha]^T$. First of all, the Inverse Kinematic is addressed, where $\mathbf{\Theta}$ is determined for a given $\mathbf{X}$. Since 3PRRR is a kinematically redundant manipulator, the mechanism has more degrees of freedom (6) than the end-effector. As a consequence, for a given (x, y, α), actuators positions $(\zeta_1, \zeta_2, \zeta_3, \theta_1, \theta_2, \theta_3)$ are undetermined. For this reason, it is assumed that $(\zeta_1, \zeta_2, \zeta_3)$ are previuosly determined (how this it can be done is discussed in section 3). Thus, the current goal is to find $(\theta_1, \theta_2, \theta_3)$ for known $(\zeta_1, \zeta_2, \zeta_3, x, y, \alpha)$.

To do so, kinematic contraints of a chain i is written eliminating β_i through the following equation:

$$||\mathbf{r}_{\mathbf{C_i}} - \mathbf{r}_{\mathbf{B_i}}||^2 = \left\| \begin{bmatrix} \rho_{xi} - l_2 \cos\theta_i \\ \rho_{yi} - l_2 \sin\theta_i \end{bmatrix} \right\|^2 = l_3^2 \tag{1}$$

where

$$\begin{bmatrix} \rho_{xi} \\ \rho_{yi} \end{bmatrix} = \begin{bmatrix} x \\ y \end{bmatrix} + h \begin{bmatrix} \cos(\alpha + \gamma_i \pm {}^{\pi}/_{2}) \\ \sin(\alpha + \gamma_i \pm {}^{\pi}/_{2}) \end{bmatrix} - \zeta_i \begin{bmatrix} \cos\gamma_i \\ \sin\gamma_i \end{bmatrix} - a \begin{bmatrix} \cos(\gamma_i \pm {}^{\pi}/_{2}) \\ \sin(\gamma_i \pm {}^{\pi}/_{2}) \end{bmatrix} \tag{2}$$

Vector $\mathbf{r}_{\mathbf{OA_i}}$ are written as $a\,[\cos(\gamma_i \pm {}^{\pi}/_{2})\ \sin(\gamma_i \pm {}^{\pi}/_{2})]^T$ because its length is a and its orientation is perpendicular to the respective linear actuator given by γ_i. The signal of $\pm {}^{\pi}/_{2}$ is defined in function of the direction of increasement of ζ_i. For the specific case of Fig. 2, the angle is $\gamma_i + {}^{\pi}/_{2}$. The same rationale is employed for the vector which is the second parcel on the right-hand of (2).

Expanding the norm in (1)

$$\underbrace{-2.l_2.\rho_{yi}}_{e_{1i}} \sin\theta_i + \underbrace{-2.l_2.\rho_{xi}}_{e_{2i}} \cos\theta_i + \underbrace{\rho_{xi}^2 + \rho_{yi}^2 + l_2^2 - l_3^2}_{e_{3i}} = 0 \tag{3}$$

The transcendental equation (3) may be solved analytically θ_i with the *Weierstrass substitution* transforming trigonometric functions of θ_i in functions of $\tan\left({}^{\theta_i}/_2\right)$.

$$\theta_i = 2\tan^{-1}\left(\frac{-e_{i1} \pm \sqrt{e_{i1}^2 + e_{i2}^2 - e_{i3}^2}}{e_{i3} - e_{i2}}\right) \tag{4}$$

Once θ_i is known, determing β_i is necessary. It can be deno through

$$\beta_i = \tan^{-1}\left(\frac{\rho_{yi} - l_2\ \sin\theta_i}{\rho_{xi} - l_2\ \cos\theta_i}\right) \tag{5}$$

2.1.2 Forward Kinematics

In general, available data regarding robot positions is limited to readings of $\mathbf{\Theta}$ given by encoders. This way, finding end-effector positions $\mathbf{X}$ for a given $\mathbf{\Theta}$ is required. This method is called Forward Kinematics. Mathematical complexity makes analytical methods difficult in this case. Therefore, this relation is attained numerically. For known ζ_i e θ_i ($i = 1, 2, 3$), equation (6) is solved numerically, defining x, y e α.

$$\left\| -h\begin{bmatrix}\cos(\gamma_i \pm {}^{\pi}/_2)\\ \sin(\gamma_i \pm {}^{\pi}/_2)\end{bmatrix} - \begin{bmatrix}x\\ y\end{bmatrix} + a\begin{bmatrix}\cos(\gamma_i \pm {}^{\pi}/_2)\\ \sin(\gamma_i \pm {}^{\pi}/_2)\end{bmatrix} + \zeta_i\begin{bmatrix}\cos\gamma_i\\ \sin\gamma_i\end{bmatrix} + l_2\begin{bmatrix}\cos\theta_i\\ \sin\theta_i\end{bmatrix} \right\| - l_3 = 0 \tag{6}$$

2.1.3 Jacobian Matrix

A relevant information of the manipulator for a given position is its Jacobian Matrix. It can be determined by the equation $||\mathbf{r_{BC}}||^2 = l_3^2$. Its derivative is $r_{BC_x}\,\dot{r}_{BC_x} + r_{BC_y}\,\dot{r}_{BC_y} = 0$. Position elements r_{BC_x} e r_{BC_y} are substituted by $l_3\,\cos\beta_i$ e $l_3\,\sin\beta_i$, respectively. Velocity components $\dot{r}_{BC_x}$ and $\dot{r}_{BC_y}$ are obtained differentiating (3). Thus, each kinematic chain i lead to an equation:

$$\dot{x}\,\underbrace{[l_3\cos\beta_i]}_{a_{i1}} + \dot{y}\,\underbrace{[l_3\sin\beta_i]}_{a_{i2}} + \dot{\alpha}\,\underbrace{[l_3\,h\sin(\beta_i - \gamma_i - \alpha \pm {}^{\pi}/_2)]}_{a_{i3}} = \dot{\theta}_i\,\underbrace{[l_2\,l_3\sin(\beta_i - \theta_i)]}_{b_{ii}} + \dot{\zeta}_i\,\underbrace{[l_3\cos(\beta_i - \gamma_i)]}_{b_{ii+3}} \tag{7}$$

Following the subindices as described in (7), matrices $\mathbf{A}_{3x3} = (a_{i,j})$ and $\mathbf{B}_{3x6} = (b_{i,j})$ can be assembled so that $\mathbf{X} = [x, y, \alpha]^T$ and $\mathbf{\Theta} = [\theta_1, \theta_2, \theta_3, \zeta_1, \zeta_2, \zeta_3]^T$ have their velocities correlated by

$$\begin{aligned}\mathbf{A}_{3x3}\dot{\mathbf{X}}_{3x1} &= \mathbf{B}_{3x6}\dot{\mathbf{\Theta}}_{6x1}\\ \dot{\mathbf{X}} &= \mathbf{A}^{-1}\mathbf{B}\dot{\mathbf{\Theta}}\end{aligned} \tag{8}$$

This way, the Jacobian Matrix $\mathbf{J}_{3x6}$ is calculated as $\mathbf{J} = \mathbf{A}^{-1}\mathbf{B}$. It is important to note that the occurrence of $\mathbf{A}$ or $\mathbf{B}$ with null determinant leads to singularities. The major concern regarding this matter is in cases when $\mathbf{A}$ is singular, making possible displacements of $\mathbf{X}$ with actuators locked. This situation induce a loss of rigidity of the mechanism.

2.2 Dynamic Model

Additionally to Kinematic Model, complete simulations require a Dynamic Model of the system. This section address this point, equating analytically and proposing numerical methods able to solve it. The Euler-Lagrange formalism has been used with Lagrange multiplier in order to account with kinematic constraints. The solution of a system of Differential Algebraic Equations (DAE) is necessary in the numerical integration the Forward Dynamics. A method proposed by (Brenan *et al.*, 1996) has been implemented using *Backward Differential Formula* (BDF).

2.2.1 Mass Matrix and Kinematic Energy

For a kinematic chain i, positions parameters are $\mathbf{\Theta}_i^* = [\zeta_i\ \theta_i\ \beta_i]^T$, according to Fig.2. The indication * displays that the original vector of actuators positions has been augmented with the orientation of the passive joint β_i. Each chain has three rigid bodies, which can be identified by an index j as follows: ($j = 1$) the body considered as a concentrated mass in A_i, ($j = 2$) the link $\overline{A_iB_i}$, and ($j = 3$) the link $\overline{B_iC_i}$.

Is defined a vector $\boldsymbol{\nu}_{ij}$ related to body j of chain i which presents its Cartesian and rotational velocities

$$\boldsymbol{\nu}_{ij} = \begin{bmatrix} v_{xij} \\ v_{yij} \\ \omega_{ij} \end{bmatrix} \tag{9}$$

where v_{xij} and v_{yij} are Cartesian velocities of the center of mass in x and y respectively and ω_{ij} is the angular velocity.

It is necessary to define matrices that relate $\dot{\boldsymbol{\Theta}}_i^*$ to $\boldsymbol{\nu_{ij}}$. These matrices are called partial velocity matrices denoted by $\mathbf{K}_{ij}$.

$$\begin{aligned}
\boldsymbol{\nu}_{i1} &= \underbrace{\begin{pmatrix} \cos\gamma_i & 0 & 0 \\ \sin\gamma_i & 0 & 0 \\ 0 & 0 & 0 \end{pmatrix}}_{\mathbf{K}_{i1}} \dot{\boldsymbol{\Theta}}_i^* \\
\boldsymbol{\nu}_{i2} &= \underbrace{\begin{pmatrix} \cos\gamma_i & -s_2\,\sin\theta_i & 0 \\ \sin\gamma_i & s_2\,\cos\theta_i & 0 \\ 0 & 1 & 0 \end{pmatrix}}_{\mathbf{K}_{i2}} \dot{\boldsymbol{\Theta}}_i^* \\
\boldsymbol{\nu}_{i3} &= \underbrace{\begin{pmatrix} \cos\gamma_i & -l_2\,\sin\theta_i & -s_3\,\sin\beta_i \\ \sin\gamma_i & l_2\,\cos\theta_i & s_3\,\cos\beta_i \\ 0 & 0 & 1 \end{pmatrix}}_{\mathbf{K}_{i3}} \dot{\boldsymbol{\Theta}}_i^*
\end{aligned} \tag{10}$$

where s_2 is the distance between A_i and the center of mass of link $\overline{A_iB_i}$, and s_3 is the distance between B_i and the center of mass of link $\overline{B_iC_i}$.

Let μ_j be a matrix with the parameters of a body j

$$\mu_j = \begin{pmatrix} m_j & 0 & 0 \\ 0 & m_j & 0 \\ 0 & 0 & I_j \end{pmatrix} \tag{11}$$

then T_i, the sum of kinetic energy of all bodies of the chain i is given by

$$\begin{aligned}
T_i &= \frac{1}{2} \sum_{j=1}^{3} \boldsymbol{\nu_{ij}}^T \mu_j \, \boldsymbol{\nu_{ij}} \\
&= \frac{1}{2}\, \dot{\boldsymbol{\Theta}}_i^{*T} \underbrace{\left(\sum_{j=1}^{3} \mathbf{K}_{ij}^T \, \mu_j \, \mathbf{K}_{ij} \right)}_{\mathbf{M}_i} \dot{\boldsymbol{\Theta}}_i^*
\end{aligned} \tag{12}$$

In addition, the kinematic energy of the end-effector is

$$T_N = \frac{1}{2}\, \dot{\mathbf{X}}^T \underbrace{\begin{pmatrix} m_N & 0 & 0 \\ 0 & m_N & 0 \\ 0 & 0 & I_N \end{pmatrix}}_{\mathbf{M}_N} \dot{\mathbf{X}} \tag{13}$$

In order to assess total kinematic energy, a vector $\mathbf{q} = [\boldsymbol{\Theta}_1^{*\boldsymbol{T}}\ \boldsymbol{\Theta}_2^{*\boldsymbol{T}}\ \boldsymbol{\Theta}_3^{*\boldsymbol{T}}\ \mathbf{X}^T]^T$ is defined so that

$$T = \frac{1}{2}\, \dot{\mathbf{q}}^T \, \mathbf{M} \, \dot{\mathbf{q}} \tag{14}$$

where the mass matrix $\mathbf{M}$ is assembled with submatrices $\mathbf{M}_1$, $\mathbf{M}_2$, $\mathbf{M}_3$ and $\mathbf{M}_N$ defined in (12) and (13) disposed as follows

$$\mathbf{M} = \begin{pmatrix} \mathbf{M}_1 & & & \\ & \mathbf{M}_2 & & \\ & & \mathbf{M}_3 & \\ & & & \mathbf{M}_N \end{pmatrix} \tag{15}$$

2.2.2 Dynamic Equations

Elements of vector $\mathbf{q}$ are not independent. As a result, the Lagrange Multipliers method is used. Since the mechanism has 6 degrees of freedom while $\mathbf{q}$ has 12 components, 6 constraint equations together with 6 Lagrange multipliers should be applied. Constraint equations are

$$\begin{aligned}\begin{bmatrix} g_p \\ g_{p+1} \end{bmatrix} =& a \begin{bmatrix} \cos(\gamma_i \pm {}^{\pi}/_{2}) \\ \sin(\gamma_i \pm {}^{\pi}/_{2}) \end{bmatrix} + \zeta_i \begin{bmatrix} \cos\gamma_i \\ \sin\gamma_i \end{bmatrix} + l_2 \begin{bmatrix} \cos\theta_i \\ \sin\theta_i \end{bmatrix} + \dots \\ & \dots + l_3 \begin{bmatrix} \cos\beta_i \\ \sin\beta_i \end{bmatrix} - h \begin{bmatrix} \cos(\alpha+\gamma_i \pm {}^{\pi}/_{2}) \\ \sin(\alpha+\gamma_i \pm {}^{\pi}/_{2}) \end{bmatrix} - \begin{bmatrix} x \\ y \end{bmatrix} = 0 \end{aligned} \qquad k = 2\,i \quad \{i = 1, 2, 3\} \tag{16}$$

See that each system of equations $[g_p \quad g_{p+1}]^T = 0$ represents kinematic constraints of a chain i, where $k = 2\,i$. This way, vectorial equation $\mathbf{g}_{6\text{x}1} = 0$ results in 6 algebraic equations.

Once there is not any variation of potential energy in this system (the robot moves in an horizontal plane), the lagragian is $L = T$. Calculating partial and temporal derivatives of (14) and (16), the application of the Euler-Lagrange Equation with multiplier $\boldsymbol{\lambda} = [\lambda_1\ \lambda_2\ \dots\ \lambda_6]^T$ leads to

$$\mathbf{M}_{12\text{x}12}\,\ddot{\mathbf{q}}_{12\text{x}1} + \mathbf{b}_{12\text{x}1}(\mathbf{q}, \dot{\mathbf{q}}) + \mathbf{G}^T\,\boldsymbol{\lambda} = \boldsymbol{\tau} \tag{17}$$

$$\mathbf{g}(\mathbf{q}) = 0 \tag{18}$$

where $\mathbf{G}_{6\text{x}12}$ is the jacobian matrix of the vectorial function $\mathbf{g}$, $\boldsymbol{\tau} = [\tau_1\ \tau_2\ \dots\ \tau_{12}]^T$ has components τ_k representing non conservative generalized forces acting on q_k, and $\mathbf{b}$ is calculated by

$$\mathbf{b}(\mathbf{q}, \dot{\mathbf{q}}) = \dot{\mathbf{M}}\,\dot{\mathbf{q}} - \begin{bmatrix} \frac{\partial T}{\partial q_1} \\ \frac{\partial T}{\partial q_2} \\ \vdots \\ \frac{\partial T}{\partial q_{12}} \end{bmatrix} \tag{19}$$

2.2.3 Inverse Dynamics

Knowing all positions $\mathbf{q}, \dot{\mathbf{q}}, \ddot{\mathbf{q}}$ over the time, Inverse Dynamics defines torques and forces necessary to perform such movement. The robot 3PRRR has 6 actuators: 3 linear actuating ζ and 3 rotary actuating θ. One can see that unknown variables of (17) are $\boldsymbol{\lambda}$, $\tau_1,\ \tau_2,\ \tau_4,\ \tau_5,\ \tau_7$ and τ_8 (τ_k related to ζ_i and θ_i). Lagrange multipliers $\boldsymbol{\lambda}$ are present in all 12 equations, while 6 τ_k indicated above are present only in its respective equations $k = 1, 2, 4, 5, 7, 8$. Therefore, remaining equations $k^c = 3, 6, 9, 10, 11, 12$ have $\boldsymbol{\lambda}$ as unique unknown variable. With this in mind, $\boldsymbol{\lambda}$ can be isolated inverting the square matrix containing lines k^c of $\mathbf{G}^T$. After that, k components of $\boldsymbol{\tau}$ are obtained directly.

Equating this procedure, lines $k^c = 3, 6, 9, 10, 11, 12$ are extracted from (17) (see that $\tau_{k^c} = 0$ when there is not any non conservative force in this components, that is to say, when these are frictionless passive joints)

$$\begin{aligned} \mathbf{M}_{k^c}\,\ddot{\mathbf{q}} + \mathbf{b}_{k^c} + \mathbf{G}_{k^c}^T\,\boldsymbol{\lambda} &= 0 \Rightarrow \\ \Rightarrow \boldsymbol{\lambda} &= -(\mathbf{G}_{k^c}^T)^{-1}\,(\mathbf{M}_{k^c}\,\ddot{\mathbf{q}} + \mathbf{b}_{k^c}) \end{aligned} \tag{20}$$

Substitution of (20) in (17) leads to forces and torques required from actuators τ_k.

Non conservative generalized forces (as disturbances and friction) acting in $\beta_i,\ x,\ y$ and α can be easily added in (20) making $\tau_{k^c} \neq 0$. The simplest case where $\tau_{k^c} = 0$ has been exposed in an effort to facilitate comprehension.

2.2.4 Forward Dynamics

Forward Dynamics obtains the resulting movement $\mathbf{q}(t)$ knowing $\boldsymbol{\tau}$. This takes place through numerical integration of the system (17/18). This is a system of Differential Algebraic Equations (DAE) with order 2 and index 3 (Hairer and Wanner, 1996). First of all, it is necessary to reduce its order to 1

$$\begin{aligned} \mathbf{u} - \dot{\mathbf{q}} &= 0 \\ \mathbf{M}\,\dot{\mathbf{u}} + \mathbf{b}(\mathbf{q}, \mathbf{u}) + \mathbf{G}^T\,\boldsymbol{\lambda} - \boldsymbol{\tau} &= 0 \\ \mathbf{g}(\mathbf{q}) &= 0 \end{aligned} \tag{21}$$

In order to integrate (21), *Backward Differential Formula* (BDF) has been used. This can approximate the derivatives $\dot{\mathbf{q}}(t_n)$ and $\dot{\mathbf{u}}(t_n)$ in a given instant t_n considering $\mathbf{q}$ and $\mathbf{u}$ calculated in previous steps. This way, unknown variables

in (21) becomes $\mathbf{q}(t_n)$, $\mathbf{u}(t_n)$ and $\boldsymbol{\lambda}(t_n)$. Therefore, it can be solved as a purely algebraic system for each step. To do so, algorithm Trust Region Dogleg (built in MATLAB) has been used with the analytical jacobian matrix of the related system of algebraic equations.

It is noteworthy to say that this method is able to easily simulate disturbances and friction actuating in any part of the manipulator and control actions applied in an effort to suppress errors

3. MOTION PLANNING

For a given pose of the end-effector, the kinematic redundancy yield to undetermined actuators positions. Using this idea, the present section focuses on the following problem: given an end-effector path $\mathbf{X}(t)$, define a convenient $\boldsymbol{\Theta}(t)$.

A leading function $\phi(\boldsymbol{\zeta}, t)$, dependent on redundant actuators positions $\boldsymbol{\zeta}$ and the time, is defined so that it is maximized for advantageous configurations at each instant t. Redundant actuators motion is defined according to the following differential equation:

$$\ddot{\boldsymbol{\zeta}} = \nabla\phi(\boldsymbol{\zeta}) + \boldsymbol{\Gamma}(\boldsymbol{\zeta}, \dot{\boldsymbol{\zeta}}) \tag{22}$$

where $\nabla\phi(\boldsymbol{\zeta})$ is the gradient of ϕ for a fixed t. This term generates main accelerations directing $\boldsymbol{\zeta}$ towards the maximum of ϕ, and $\boldsymbol{\Gamma}$ generates secondary accelerations responsible for maintaining $\boldsymbol{\zeta}$ into the feasible amplitude of the linear actuators and to guarantee convergence towards the maximum of ϕ. Once a proper ϕ is defined, the nature of Eq.22 imposes that redundant actuators are continuously seeking a convenient position, measured by $\phi(\boldsymbol{\zeta})$.

Motion planning is performed through the numerical integration of Eq. 22. Many choices of ϕ and $\boldsymbol{\Gamma}$ are possible. Results presented in the next section are obtained with ϕ based mainly on singular values extracted from $\mathbf{J}$, while $\boldsymbol{\Gamma}$ simulates dampers located in the extreme point of each linear actuator.

4. RESULTS

Methods described in last sections are implemented in order to evaluate differences between performances of a non-redundant 3RRR and a redundant 3PRRR. Obviously, model developed to the redundant case can be used to simulate 3RRR using $\boldsymbol{\zeta} = \mathbf{0}$.

Parameters of the simulated robot are displayed in tables 1 and 2. Moments of inertia of links A_iB_i and B_iC_i have were considered as if these bodies were simple rods.

Table 1: Dimensions of the robot

h	a	ζ_{max}	l_2	l_3	γ_1	γ_2	γ_3
59.7 mm	259.8 mm	249.2 mm	191 mm	232 mm	-180°	60°	-60°

Table 2: Masses and moment of inertia

m_{i1}	m_{i2}	m_{i3}	m_n	I_n
0.6 kg	0.16 kg	0.13 kg	0.25 kg	0.002 kg.m^2

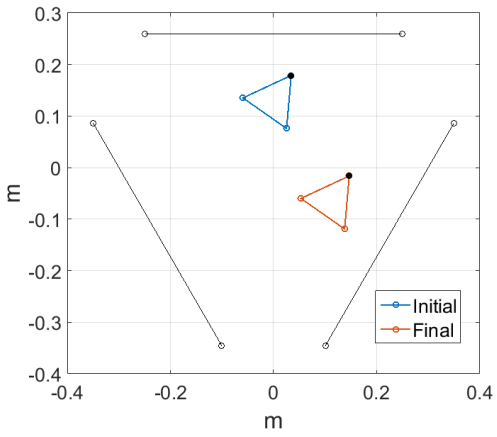

Figure 3: Localization in the workspace of initial and final positions of the simulated trajectory

The trajectory is a typical pick-and-place task, in which the end-effector performs through a straight line the transport of some object from its initial position to the final position. Accelerations and velocities in these limiting positions are null. Figure 3 shows initial and final poses located into the workspace. Movement is done in 0.3 second and the simulation is continued over 0.9 second in order to make possible the evaluation of the following response.

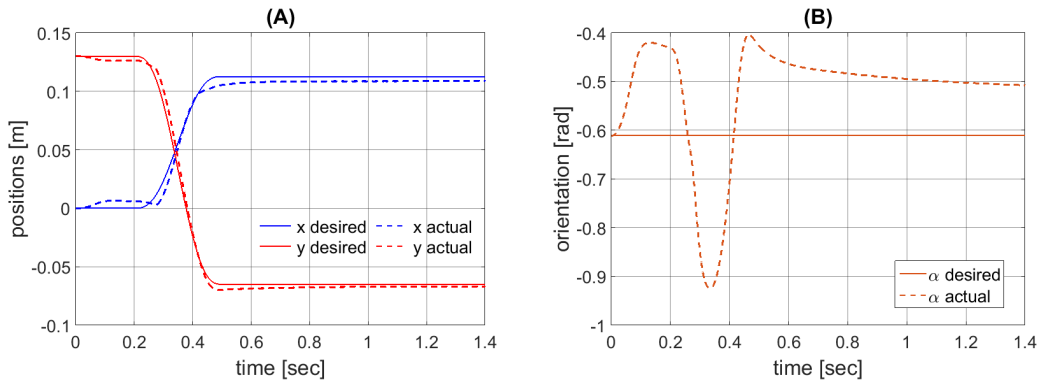

Figure 4: (A) Positions and (B) orientation (desired and actual) of the **non-redundant** robot

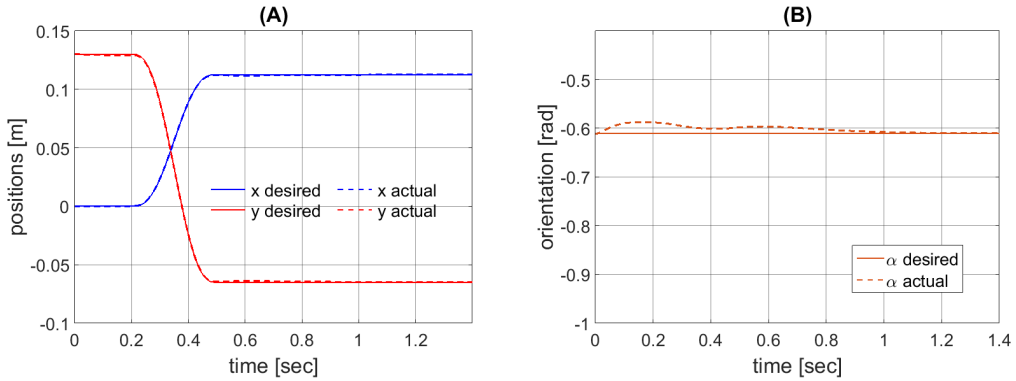

Figure 5: (A) Positions and (B) orientation (desired and actual) of the **redundant** robot

As described earlier, disturbances and control action can be simulated. In an effort to clarify how the mechanism can respond under unpredicted forces, a torque of 0.2 N.m is applied about the center of the end-effector. With the purpose of suppressing the action of such torque, a PID controller is programmed based on position errors read by each actuator. Parameters of this controller are in table 3

Table 3: Controller parameters

Linear			Rotary		
P	I	D	P	I	D
3360	8774	218	113.4	46.7	12.3

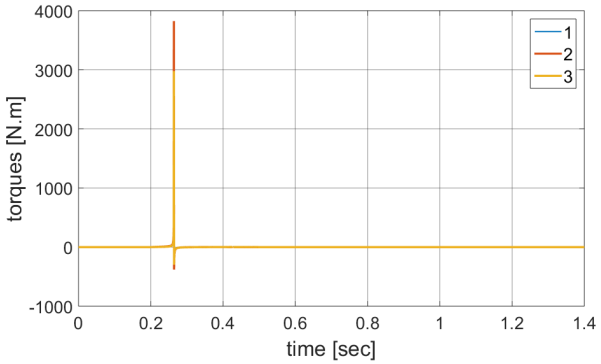

Figure 6: Torques of the **non-redundant** robot

One can see through Fig. 4 that the non-redundant 3RRR performs a poor trajectory, with considerable errors in positioning, mainly in α. This is a consequence of the fact that the trajectory intersects a singularity where $det(\mathbf{A}) = 0$, causing loss of rigidity of the mechanism (see subsection 2.1.3). Another manifestation of this phenomenon is the atypical value of torques achieving more than 3500 N.m when $t \approx 0.26$ seconds (Fig. 6). Obviously, real actuators are not able to perform this loads predicted by the Inverse Dynamics.

On the other hand, if kinematic redundancy is applied, the manipulator becomes able to reconfigure itself, enhancing the rigidity of the mechanism for a given trajectory. As a result, it can be seen in Fig. 5 that desired and actual positions stay close to each other and error tends to zero as the simulations is continued. Similarly, forces and torques take reasonable values, as depicted in Fig. 7.

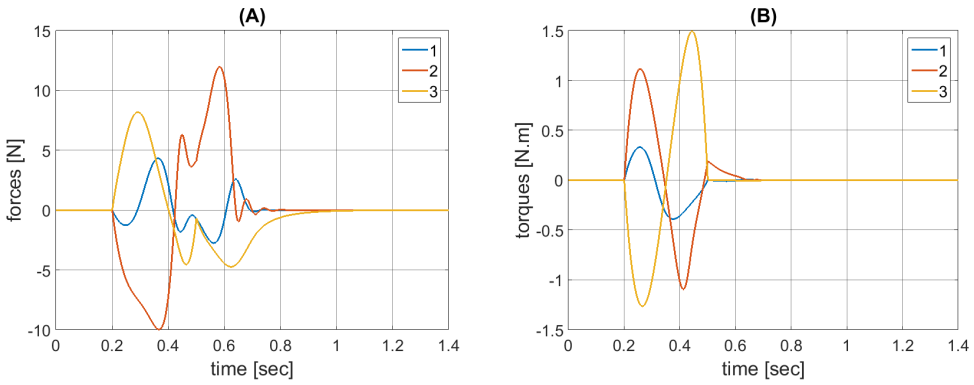

Figure 7: (A) Forces and (B) torques of the **redundant** robot

5. CONCLUSIONS

Methods proposed in section 2 have been shown to be a efficient and simple way of modeling robots 3RRR and 3PRRR. It is possible to obtain necessary loads for a given trajectory through Inverse Dynamics and simulate effects of any kind of disturbance, friction and control action. This is because a formulation with more variables of positions (12 in total) facilitate the determination of generalized forces acting in different point of the manipulator.

In addition, the main presented result is the improvement on the performance of a PKM obtained thanks to kinematic redundancy. Simulations in section 4 demonstrate that singularities can be suppressed. Furthermore, as a result of increased rigidity, the mechanism susceptibility under disturbances is enhanced.

6. ACKNOWLEDGEMENTS

This research is supported by FAPESP 2014/01809-0 and FP7-EMVeM (Energy Efficiency Management for Vehicles and Machines). Moreover, João C. Santos is grateful for their grant FAPESP 2014/21946-2.

7. REFERENCES

Bonev, I.A., Zlatanov, D. and Gosselin, C.M., 2003. "Singularity Analysis of 3-DOF Planar Parallel Mechanisms via Screw Theory". *Journal of Mechanical Design*, Vol. 125, No. 3, pp. 573–581. ISSN 1050-0472. doi: 10.1115/1.1582878.

Brenan, K.E., Campbell, S.L. and Petzold, L.R., 1996. *Numerical solution of initial-value problems in differential-algebraic equations*, Vol. 14. Siam. ISBN 1611971225.

Briot, S. and Bonev, I., 2007. "Are parallel robots more accurate than serial robots?" *CSME Transactions*, Vol. 31, No. 4, pp. 445–456.

Corbel, D., Gouttefarde, M., Company, O. and Pierrot, F., 2010. "Towards 100G with PKM. Is actuation redundancy a good solution for pick-and-place?" In *Robotics and Automation (ICRA), 2010 IEEE International Conference on*. IEEE, pp. 4675–4682. ISBN 1424450381.

Ebrahimi, I., Carretero, J.A. and Boudreau, R., 2007. "3-PRRR redundant planar parallel manipulator: Inverse displacement, workspace and singularity analyses". *Mechanism and Machine Theory*, Vol. 42, No. 8, pp. 1007–1016. ISSN 0094-114X.

Gogu, G., 2007. "Structural synthesis of fully-isotropic parallel robots with Schönflies motions via theory of linear transformations and evolutionary morphology". *European Journal of Mechanics-A/Solids*, Vol. 26, No. 2, pp. 242–269. ISSN 0997-7538.

Gosselin, C. and Angeles, J., 1990. "Singularity analysis of closed-loop kinematic chains". *Robotics and Automation, IEEE Transactions on*, Vol. 6, No. 3, pp. 281–290. ISSN 1042-296X. doi:10.1109/70.56660.

Hairer, E. and Wanner, G., 1996. "Solving ordinary differential equations ii: Stiff and differential-algebraic problems second revised edition with 137 figures". *Springer series in computational mathematics*, Vol. 14. ISSN 0179-3632.

Kock, S. and Schumacher, W., 1998. "A parallel xy manipulator with actuation redundancy for high-speed and active-stiffness applications". In *Robotics and Automation, 1998. Proceedings. 1998 IEEE International Conference on*. IEEE, Vol. 3, pp. 2295–2300. ISBN 078034300X.

Merlet, J.P., 2012. *Parallel robots*, Vol. 74. Springer Science & Business Media. ISBN 9401095876.

Rocha, D.M. and da Silva, M.M., 2013. "Workspace and singularity analysis of redundantly actuated planar parallel kinematic machines". In *Proc. of the XV International Symposium on Dynamic Problems of Mechanics, Búzios, RJ, Brazil*. pp. 1–10.

Stewart, D., 1965. "A platform with six degrees of freedom". *Proceedings of the institution of mechanical engineers*, Vol. 180, No. 1, pp. 371–386. ISSN 0020-3483.

Wenger, P. and Chablat, D., 2007. "Design of a three-axis isotropic parallel manipulator for machining applications: The orthoglide". *arXiv preprint arXiv:0705.1282*.